Article

Adsorption of Sunscreen Compounds from Wastewater Using Commercial Activated Carbon: Detailed Kinetic and Thermodynamic Analyses

Stefania Gheorghe *,†, Vasile Ion Iancu, Ioana Alexandra Ionescu, Florinela Pirvu, Iuliana Claudia Paun †, Luoana Florentina Pascu and Florentina Laura Chiriac *

National Research and Development Institute for Industrial Ecology—ECOIND,
Drumul Podu Dambovitei Street 57-73, 060652 Bucharest, Romania; vasile.iancu@incdecoind.ro (V.I.I.);
ioana.ionescu@incdecoind.ro (I.A.I.); florinela.pirvu@incdecoind.ro (F.P.); iuliana.paun@incdecoind.ro (I.C.P.);
ecoind@incdecoind.ro (L.F.P.)
* Correspondence: stefania.gheorghe@incdecoind.ro (S.G.); laura.chiriac@incdecoind.ro (F.L.C.)
† These authors contributed equally to this work.

Abstract: Sunscreen compounds are one of the most toxic substances detected in the aqueous environment. However, these molecules are continuously utilized in a various range of products to provide protection against UV radiation. The removal of three sunscreen compounds, 4-hydroxybenzophenone (**4-HBP**), 2,4-dihydroxybenzophenone (**BP-1**) and oxybenzone (**BP-3**), by commercial activated carbon (AC) was investigated using batch adsorption experiments. Different operational characteristics, such as adsorbent dosing, interaction time, solution pH and starting sunscreen compound concentration, were studied. The adsorption capacity of the AC material was assessed using a liquid chromatograph associated with a mass spectrometer detector (LC–MS/MS). Two isotherm models were utilized to explained the target compound adsorption phenomenon (Langmuir and Freundlich), while pseudo-first and -second kinetic orders and thermodynamics were utilized to examine the adsorption mechanism. The maximum adsorption capacities determined from the Langmuir isotherms were established as 43.8 mg/g for **4-HBP**, 48.8 mg/g for **BP-3** and 41.1 mg/g for **BP-1**. The thermodynamic parameters revealed the following: a negative $\Delta G°$ (<20 KJ/mol) and $\Delta H°$ and a positive $\Delta S°$ of the targeted sunscreen compounds adsorbed onto AC suggest a spontaneous and exothermic adsorption process, favored by lower temperature, proving that the physical sorption mechanism prevailed. Effective adsorption of **4-HBP**, **BP-3** and **BP-1** from real wastewater samples proved the viability of sunscreen compound removal using commercial AC material. This paper offers promising results on a sustainable, economical and environmentally friendly method for removal of ubiquitous sunscreen compounds from wastewater, as a possible enhancement of treatment processes.

Keywords: benzophenone-type sunscreen compounds; activated carbon; removal efficiencies; adsorption study; kinetics; thermodynamic characteristics

1. Introduction

Sunscreen compounds are a class of chemicals extensively used in all kinds of cosmetic products to prevent the skin, lips and hair from getting UV irradiation damage [1]. In addition, sunscreens are indispensable components in different color and plastic products for obstructing UV degradation [2]. Benzophenones (BPs) are the most representative class of sunscreen, used worldwide in various products [3]. As a consequence, many BPs and similar compounds have been released into aquatic ecosystems via direct (by the practices of water sports and bathing) or indirect sources (effluents discharged into natural water bodies) [4,5]. This type of pollution of water resources represents a significant issue for both

aquatic environments and human health, with many BPs being known to pose endocrine disruptor characteristics [6,7].

Considering the previously mentioned information, solutions to improving the removal of these contaminants in WWTPs are imperative. Treatment processes that are usually applied for the elimination of organic contaminants from aqueous media involve adsorption [8–10], photocatalytic degradation [11] or conventional/advanced oxidation processes [12]. Although conventional/advanced oxidation processes are highly efficient candidates for the removal of organic pollutants, oxidation intermediates and by-products (bromate or halogenated organic compound) are formed during oxidation processes that use ozone [13] and chlorine [14].

Adsorption is a common and extensively used technique to remove organic pollutants from aqueous media due to its simple operational mode, economic advantages (low cost) and low energy consumption [15]. The widely utilized adsorbent material for the elimination of different classes of organic compounds from aqueous systems, such as personal care products [16,17], endocrine disruptors [18], pharmaceuticals [17,19] and synthetic dyes [20], is activated carbon (AC). It is significant to mention that the adsorption process can be applied to treat water matrices contaminated with organic pollutants with different water solubilities (hydrophilic and lipophilic) [21,22]. The distinctive and flexible adsorptive capacity of AC arising from its particular surface properties (porosity, great surface reactivity for different contaminants and broad surface/volume reports), mixed with its commercial existence and accessible price, has made it an extensively used material for the elimination of different pollutants, even at extremely low levels, from water matrices [23]. Furthermore, unlike other advanced technologies, activated carbon material can eliminate diver-type chemical contaminants without leading to any other dangerous transformation products [24–26].

Although the literature abounds with studies on the removal of organic contaminants, such as pharmaceuticals [17,19], personal care products [17], organic dyes [20] and endocrine disruptors [18], from aqueous matrices using activated carbon, very few studies have focused on the removal of organic compounds such as UV filters (sunscreens). The few works reported around the world have focused in particular on a small number of compounds from the class of sun protection creams, specifically targeting oxybenzone [15,27–30] and sulisobenzone (BP-4) [29].

In Romania, benzophenone-type UV filters proved to be determined at concerning levels in wastewater treatment plants (WWTPs) and aquatic environments, due to their poor removal efficiencies in WWTPs and the transfer of partially treated wastewater into water bodies via effluent discharges [30]. Thus, 4-hydroxybenzophenone (**4-HBP**), 2,4-dihydroxybenzophenone (**BP-1**) and oxybenzone (**BP-3**) were the most popular benzophenone-type sunscreens detected in both wastewater and surface water samples. In effluents, the concentrations of the discussed compounds ranged between 12.7 and 79 ng/L for **4-HBP**, 22.9 and 181 ng/L for **BP-1**, and 6.62 and 23 ng/L for **BP-3**. In surface water, the concentration values were up to 159 ng/L for **4-HBP**, up to 206 ng/L for **BP-1** and up to 52 ng/L for **BP-3**. Evaluating the possible ecological risk for different aquatic organisms, the results showed that **BP-1** could pose a high risk for fish species, while **BP-3** could pose a low risk for freshwater algae [30].

Thus, the improvement in treatment processes in WWTPs, for their complete removal, is an important issue. The present paper represents a study conducted to examine the viability of utilizing environmentally friendly reduced-price adsorbent material, such as commercial activated carbon, to eliminate three benzophenone-type sunscreens (**4-HBP**, **BP-3** and **BP-1**) from wastewater. The proposed commercially available AC was successfully applied in two recent studies for the elimination of four pharmaceutical compounds (ibuprofen, acetaminophen, diclofenac and ketoprofen) and one synthetic dye (methyl orange) from aqueous samples [20,21]. To achieve higher removal rates, different adsorption parameters were optimized (aqueous medium pH, interaction time, adsorbent dosage and concentration of the target sunscreens). The experimental adsorption results were used
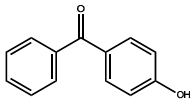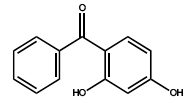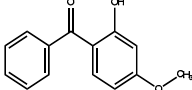
to assess Freundlich and Langmuir adsorption isotherms and kinetic (pseudo-first-order, PFO, and pseudo-second-order, PSO) and thermodynamic models. The batch adsorption investigation was widened to eliminate three sunscreen compounds from real wastewater samples. Analytical determination of the target sunscreens was effectuated using LC–MS/MS technique. The data obtained through this research will concur with the progress of capable and sustainable processes for the treatment of contaminated wastewaters with the targeted compounds, thus decreasing the environmental consequences. As far as we are aware, no scientific report on the removal of target benzophenone-type sunscreens from aqueous media using activated carbon has been published until now.

2. Materials and Methods

2.1. Chemicals

Analytical standards, **4-HBP** (>98%), **BP-1** (>98%), **BP-3** (>98%), acetonitrile (ACN, HPLC-grade), methanol (MeOH, HPLC-grade) and formic acid (FA), were purchased from Sigma-Aldrich (Darmstadt, Germany). Physical–chemical properties of the target sunscreens are given in Table 1. Ultrapure water was obtained in-house using a Millipore Milli-Q (Millipore, Darmstadt, Germany). The initial stock solutions were performed using ultrapure water with 5% of MeOH. The AC material was provided by Trace Elemental Instruments (Delft, The Netherlands).

Table 1. Physical–chemical properties of the three sunscreen chemicals.

Compound	Abbreviation	Molecular Formula	Molecular Weight	Solubility (mg/L)	Log Know [a]	pKa	Chemical Structure
4-hydroxybenzophenone	**4-HBP**	$C_{13}H_{10}O_2$	198.2	405.8	3.07	8.14	
2,4-dihydroxybenzophenone	**BP-1**	$C_{13}H_{10}O_3$	214.2	413.4	2.96	7.72	
2-hydroxy-4-methoxy-benzophenone (oxybenzone)	**BP-3**	$C_{14}H_{12}O_3$	228.2	68.56	3.52	7.56	

Note: [a] Log Kow–EPI Suite™ developed by EPA.

2.2. AC Material Characterization

Adsorption experiments were performed on a commercial AC (14.7 Å pore size, 10–50 μm particle size, 870 m²/g total pore area and 256 m²/g specific surface area). The surface morphology of the AC material was analyzed using scanning electron micrograph Quanta 250 FEG equipment (Thermo Fisher Scientific, Waltham, MA, USA). Fourier-transform infrared (FTIR) spectra of the AC were recorded in the range of 4400–400 cm^{-1}, utilizing a FTIR BX II PerkinElmer spectrophotometer (Waltham, MA, USA).

2.3. Batch Adsorption Study

The adsorption studies were effectuated utilizing the batch method. Erlenmeyer flasks with a 100 mL capacity were utilized to prevent contamination. The effects of solution pH, interaction period, adsorbent amount and starting sunscreen concentration were studied. All samples were stirred at 120 rpm using an automatic stirrer, at 25 ± 2 °C. The experiments were performed using 150 mL of 4-HBP, BP-3 or BP-1 solutions, pH values (1, 3, 5, 7, 9, 11), interaction times (1, 2, 4, 6, 8, 10, 15, 20, 24 h), adsorbent dosages (0.005, 0.01, 0.015, 0.02, 0.025, 0.03, 0.04, 0.05 g) and initial sunscreen concentrations (1, 2.5, 5, 10, 25, 30, 50, 75 mg/L). An amount of 0.025 g of AC was added to a 150 mL conical flask at pH 7 and 120 rpm for 10 h and utilized for adsorption equilibrium experiments. All tests were effectuated in replicate (n = 3). The experimental solutions were centrifuged at

7000 rpm, and the concentrations of sunscreens in the supernatant were analyzed using the LC–MS/MS technique. The adsorption capacity for the target analyte uptake, q_e (mg/g), the amount removed and the distribution coefficient, kd, were established using the following equations:

$$\%R = \frac{C_0 - C_t}{C_0} \times 100 \tag{1}$$

$$Q_e = \frac{C_0 - C_e \times V}{m} \tag{2}$$

$$K_d = \frac{Q_e}{C_e} \tag{3}$$

where C_0 is the sunscreen starting concentration (mg/L); C_e is the sunscreen equilibrium concentration (mg/L); V is the solution volume (L); m is the AC amount (g); and Q_e is the amount of the sunscreen adsorbed (mg) per unit of AC (g).

2.4. Adsorption Isotherms

To understand the adsorption mechanisms, an investigation of the interactions between the adsorbents and the adsorbates through adsorption isotherm models was performed. The isotherm models (Langmuir and Freundlich), utilized to analyze the behavior of 4-HBP, BP-1 and BP-3 adsorption on the AC, are described by the following equations:

$$Q_e = \frac{Q_m \times K_L \times C_e}{1 + K_L \times C_e} \tag{4}$$

$$Q_e = K_F \times C_e^{1/n} \tag{5}$$

where Q_e is the amount of sunscreen adsorbed at equilibrium (mg/g); Q_m (mg/g) is the highest monolayer adsorption capacity (mg/g); K_L is the equilibrium constant (L/mg); and n and K_F are the Freundlich constants, where 1/n represents the heterogeneity factor (n > 1 represents favorable adsorption).

For the Langmuir model, the adsorption properties could be evaluated using the equilibrium parameter, R_L [31]:

$$R_L = \frac{1}{1 + C_0 \times K_L} \tag{6}$$

where R_L is the type of the isotherm that is favorable if $R_L > 1$, linear if $0 < R_L < 1$ or reversible if $R_L = 0$.

2.5. Kinetic Study

To predict the adsorption dynamics, the study's results were plotted to PFO and PSO kinetic models, described by Equations (7) and (8) [32]:

$$Ln(Q_e - Q_t) = LnQ_e - k_1 \tag{7}$$

$$\frac{t}{Q_t} = \frac{1}{k_2 \times Q_e^2} + \frac{1}{Q_e} \tag{8}$$

where k_1 (L/mg) is the constant associated with the affinity of the binding sites and k_2 (g/mg/h) is the rate constant of the PSO kinetics.

2.6. Thermodynamic Study

Thermodynamic parameters were estimating using the Langmuir isotherm model. Thus, the Gibbs energy (ΔG°), enthalpy (ΔH°) and entropy changes (ΔS°) were described using Equations (9)–(11):

$$\Delta G^{\circ} = -R \times T \times LnK_L^{\circ} \tag{9}$$

$$LnK_L^{\circ} = \frac{\Delta S^{\circ}}{R} - \frac{\Delta H^{\circ}}{R \times T} \tag{10}$$

$$\Delta G^{\circ} = \Delta H^{\circ} - T \times \Delta S^{\circ} \tag{11}$$

R (8.314 J/mol K) is the universal gas constant and T (K) is the absolute temperature.

2.7. Sunscreen Analysis

Analytical studies were performed using LC–MS/MS technique (LC Agilent 1260 and MS Agilent 6410B; Agilent, Waldbronn, Germany). Individual methods, derived from published methods [33,34], were used for the quantitation of the three sunscreen compounds. All experiments were performed using a Luna C18 chromatographic column (150 × 2.0 mm, 3.0 μm, Phenomenex, California, USA), kept at 30 °C. Total amounts of 0.15% of FA in high-purity water (A) and ACN (B) 40/60 *v/v* (for 4-HBP and BP-1) and 20% (A)/80% (B) for BP-3 were used as the mobile phase, eluted in isocratic mode (0.2 mL/min, flow rate, and 10 μL, injection volume). Quantification of **4-HBP**, **BP-3** and **BP-1** concentrations was performed in multiple reaction monitoring (MRM) operation mode. The electrospray ionization source (ESI) was utilized in negative mode for 4-HBP and BP-1 and in positive mode for BP-3. MRM transitions and the MS parameter values, such as the cell accelerator voltage (CAV), collision energy (CE), fragmentor voltage (FV) and dwell time, are presented in Table 2. ESI parameter values were the following: nebulizer pressure (40 psi), drying gas temperature (300 °C), capillary voltage (5000 V) and drying gas flow (8 L/min). The chromatographic run times were lower than 10 min for all three compounds.

Table 2. MRM and MS operational parameters.

Sunscreen Compound	Retention Time (min)	MRM Transition	FV (V)	CE (V)	CAV (V)	Dwell Time (ms)	ESI Mode
BP-3	3.75	229→151	135	20	1	250	Positive
4-HBP	7.12	197→92.0	150	45	5	250	Negative
BP-1	9.74	213→135	130	20	4	250	Negative

2.8. QA and QC

All experiments were made in triplicate, with their relative standard deviation (RSD) values being situated between 4.8 and 9.6%. A linear domain plotted between 0.05 and 10 mg/L was obtained with correlation coefficients higher than 0.999. All samples were diluted using high-purity water, to fit in the calibration domain. Blank and control samples (solutions with AC and solutions of the sunscreen compounds without AC) were used during the experiments. Blank samples and analytical standards were analyzed at each sample batch. The limits of quantitation (LOQs) were established at 0.05 mg/L for all three sunscreen compounds.

3. Results

3.1. Adsorbent Material Characterization

The surface morphology of the AC was evaluated using scanning electron microscopy (Figure 1). The SEM images show visible porosity on the surface of the AC materials. A

porous structure was observed on the AC surface, and there was a high expectation that the sunscreen molecules would get caught and adsorbed into these pores.
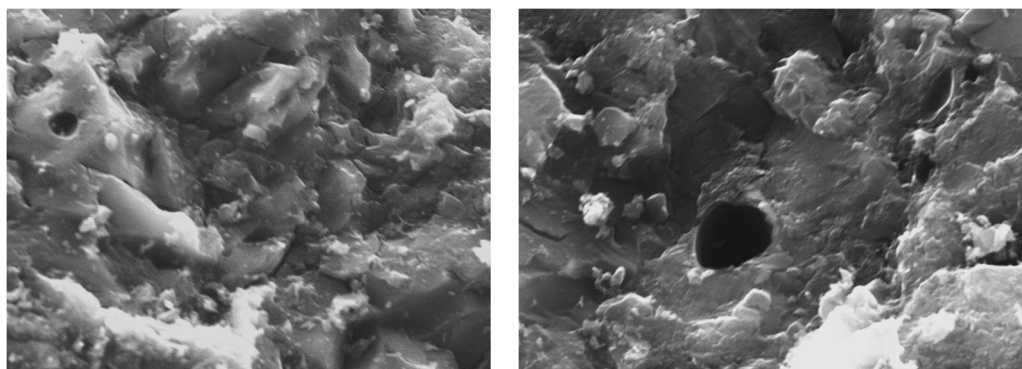

Figure 1. SEM images recorded at 10 μm (the black hole represent the macropores).

The functional groups occurring at the AC surface, which sustained the adsorption processes, were evaluated utilizing FTIR spectroscopy (Figure 2). Besides porosity, the adsorption capacity of the AC materials was also influenced by the chemical reactivity that existed on the surface. To understand the AC adsorption capacity, the functional groups on the surface of the materials were evaluated. The AC spectrum identified the existence of a ν(–OH) group around the region 3700 cm^{-1}. The methylene groups, ν(–CH$_3$/–CH$_2$), were recognized at wavenumbers situated around 2920 cm^{-1}. The functional group of ν(–O–CH$_3$) was observed at approximatively 2850 cm^{-1}. The bands situated at 2258–2352.63 cm^{-1} suggest the presence of a ν(–C≡C–) stretching vibration. The occurrence of aromatic rings could be confirmed by the band at 1534 cm^{-1} and assigned to ν(–C=C–) in the ring structure. The carboxyl or carbonyl peaks at 1496–1293 cm^{-1} revealed possible involvement of these functional groups in adsorption. The presence of the detected peaks demonstrated that the activated carbon contained plentiful functional groups able to interact with the targeted sunscreen in order to retain them on the AC surface.
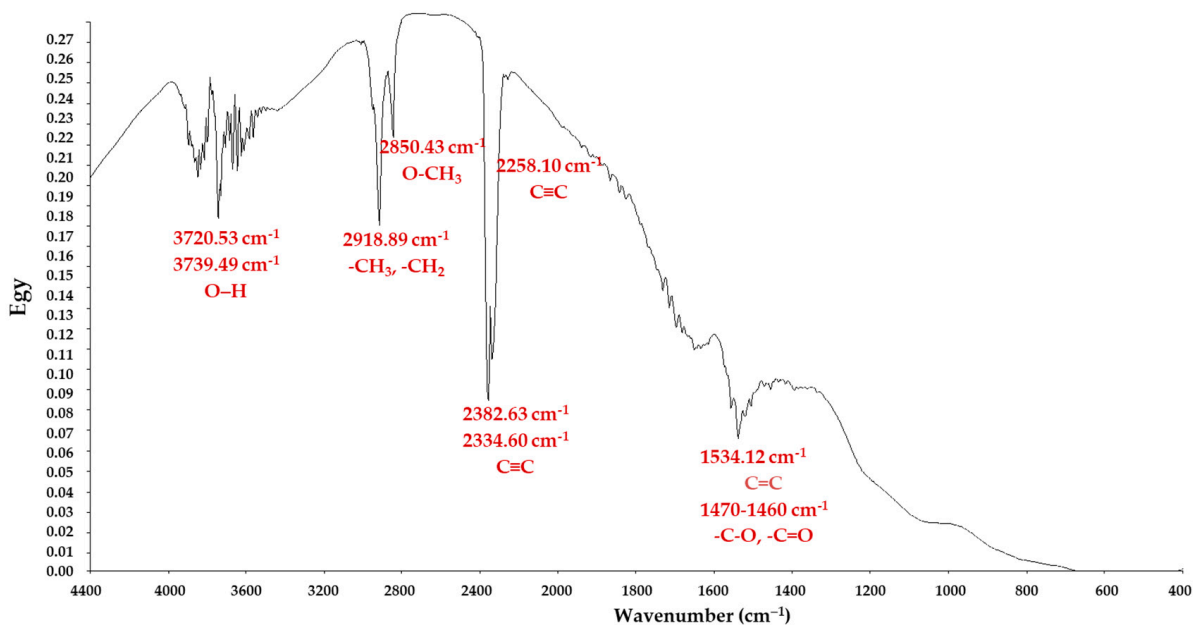

Figure 2. FTIR spectrum of AC recorded between 4400 and 400 cm^{-1}.

3.2. Optimization of Adsorption Parameters

Figure 3a presents the curves during the determination of the pHzpc of the AC and the value proved to be 8.14. At this value, the electrical charge density on the activated carbon surface was zero. Determination of the pHzpc represented a necessary step used to describe the effectiveness of the adsorption process. When pH > pHzpc, the AC surface was negatively charged, and when pH < pHzpc, the AC surface was positively charged [35]. The solution pH gives information on what happened with the AC surface during the adsorption process.
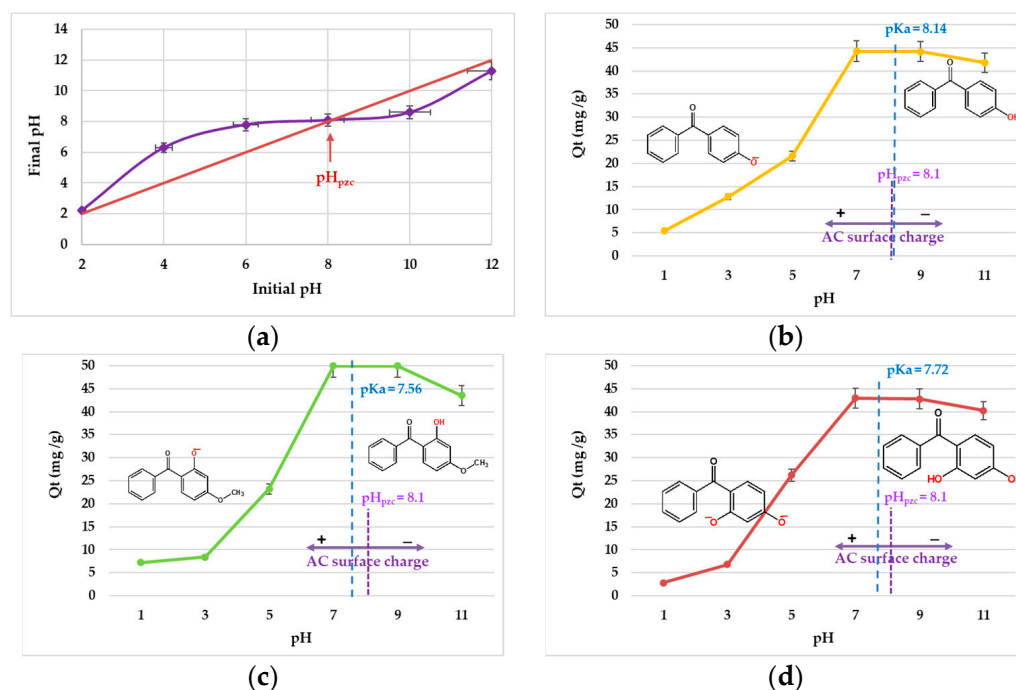

Figure 3. pHzpc (**a**) and the influence of pH on **4-HBP** (**b**), **BP-3** (**c**) and **BP-1** (**d**) adsorption onto AC (initial concentration, 25 mg/L; interaction time, 10 h; agitation speed, 125 rpm; dose of AC, 0.025 g; volume, 50 mL; temperature, 25 °C).

The uptake of the target sunscreens onto AC was performed under various pH values and illustrated in terms of adsorption capacity for every chemical substance (Figure 3b–d). It was noticed that with the increase in the solution pH, the adsorption capacity improved, reaching the maximum at alkaline pH. Above this value, the capacity of the compound adsorbed on AC decreased slightly.

The pKa value is also an important property that could have affected the adsorption process at different pH of the solution. For the target sunscreen compounds, the molecules existed in their neutral form at pH < pKa, in both neutral and anionic forms at pH ≈ pKa, and in anionic form at pH > pKa. If the AC material was positively charged (pH < pHzpc), and the sunscreens were in their neutral form (pH ≤ pKa), the adsorption process may have involved H-bonding, n–π and π–π interactions. On the other hand, if the AC surface was negatively charged (pH > pHzpc), as were the sunscreen molecules, electrostatic repulsion could have been involved.

The removal efficiencies of the three targeted sunscreen compounds by adsorption onto AC material was studied at room temperature and various pH values: 1, 3, 5, 7, 9 and 11. Higher pH values (pH > 11) were not taken into consideration, because the AC surface would be negatively charged (pH > pHzpc), decreasing the chances of a favorable adsorption process [32]. The pH proved to be a very important parameter in adsorption process, influencing both the adsorbent material and the adsorbate surface charges. Figure 4a shows that the binding efficiencies of **4-HBP**, **BP-3** and **BP-1** got better

when the pH was increased and reached their highest points at a neutral pH. Over this point, the removal efficiency decreased with further pH increases. The diminutions in removal efficiencies of the three sunscreen compounds at pH > 7 can be explained based on the merged effects of deprotonation and electrostatic repulsion. Similar data were communicated in a previous study for others type of compounds [32].
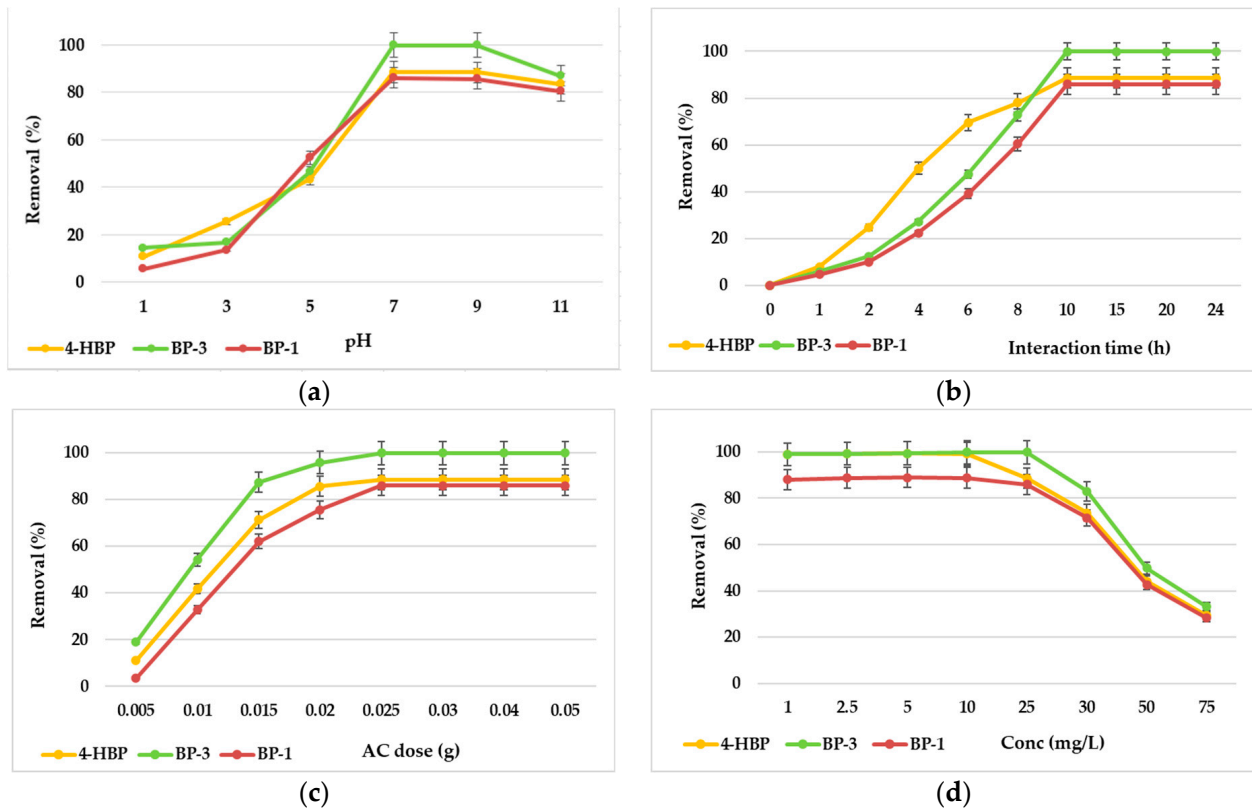

Figure 4. Effects of pH (**a**), interaction time (**b**), adsorbent dose (**c**) and initial concentrations (**d**) of sunscreen compounds on the adsorption onto AC (agitation speed, 125 rpm; temperature, 25 °C). Error bars represent standard deviations of duplicates.

Starting from the information shown in Figure 3, the mechanism of sunscreen adsorption in a neutral medium can be presented as the following (Scheme 1):
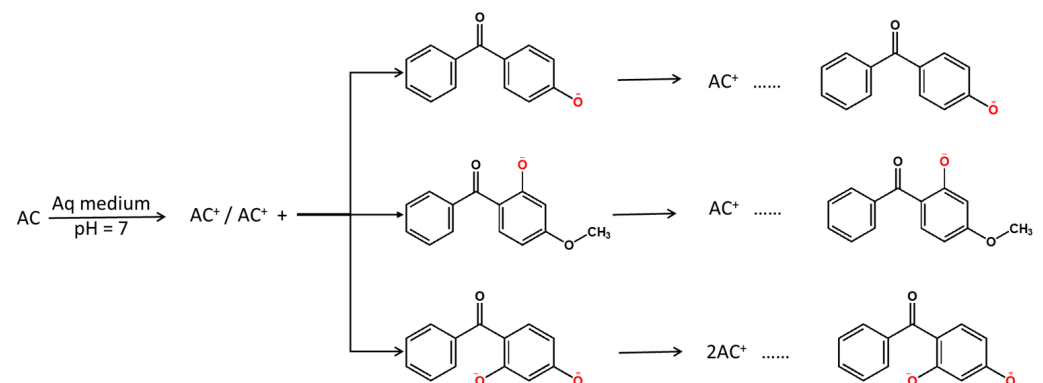
Scheme 1. **4-HBP**, **BP-3** and **BP-1** absorption mechanism onto activated carbon.

The necessary optimal interaction time was studied for the adsorption equilibria of the three sunscreen compounds on AC particles. The adsorption trials were performed at pH 7, 25 °C and with a starting compound concentration of 25 mg/L. The effects of the

interaction time for the **4-HBP**, **BP-3** and **BP-1** adsorption by the AC material are presented in Figure 4b. The maximum uptake was observed for all three studied compounds within the first 10 h. At this period, the removal efficiencies went up to 88% for **4-HBP**, up to 99% for **BP-3** and up to 86% for **BP-1**. After 10 h, the removal efficiency values remained constant. Thus, the optimal interaction time for the adsorption of targeted sunscreen compounds onto AC material was found to be 10 h.

Maintaining the sunscreen concentrations at 25 mg/L, different quantities of AC (0.005, 0.01, 0.015, 0.02, 0.025, 0.03, 0.04, 0.05 g) were added to the initial solutions to evaluate the AC dosage consequence on **4-HBP**, **BP-3** and **BP-1** adsorption. The results presented in Figure 4c show a fast increase in the adsorption data with the adsorbent amount increasing, followed by a slow increase with a further increase in the AC amount [36]. It was noticed that at 0.025 g of the AC amount, the removal efficiencies of **4-HBP**, **BP-3** and **BP-1** reached about 88.4%, 99.3% and 86.2%, respectively. Thus, 0.025 g of AC proved to be the optimal amount and was used in farther trials. The advanced rise in removal efficiency with AC amount could be explained based on the strong driving power with the rise in AC amount, leading to a uniform growth in adsorption due to the greater utilization of adsorbent dose [37]. Increasing the removal efficiency of target sunscreens with the rise in the dose of AC up to 0.025 g could be due to the rise in both the surface area of the adsorbent material and the vacant adsorption sites for the elimination of **4-HBP**, **BP-3** and **BP-1** [36]. Even so, the removal efficiencies were not improving successfully when the dose of AC was raised from 0.025 to 0.05 g. This determination could be explained by increases in the superimposition or aggregation of AC sites at a higher amount [37].

The effects of the initial **4-HBP**, **BP-3** and **BP-1** concentrations were evaluated by shaking a well-established dose of AC in sunscreen compound solutions ranging between 1 and 75 mg/L (all other parameters were maintained constant). The removal efficiency results of the target sunscreens against various starting concentration values are illustrated in Figure 4d, showing raised values from 1 mg/L to 25 mg/L. The results revealed that almost 88.6% of **4-HBP**, 99.9% of **BP-3** and 86.5% of **BP-1** removal was attained at levels between 1 and 25 mg/L. The further increased concentration levels generated reduced removal efficiencies for all three sunscreen compounds (71–28%). As the initial concentration level increased, the driving force of mass transfer increased, thus resulting in better adsorption of the sunscreen compounds. At lower values, the accessible active sites situated on the surface of the AC material to the starting sunscreen compound concentration ratio was greater; as a result, the removal of sunscreen compounds was independent of the starting concentration. At high concentration values, the percentages of the accessible active sites on the AC matter to the initial sunscreen values were low [38,39]. The decrease in the sorption of the sunscreen compounds at higher sunscreen values can be assigned to the saturation of the accessible sites, at which point the sunscreen compounds remained unabsorbed [40]. However, the phenomenon of an increase in initial concentration generating increased sunscreen compound uptake by AC could be explained by increased electrostatic interactions (physical comparative to chemical interactions) [40].

The distribution coefficients slightly increased with the increases in the initial concentrations of the sunscreens, by up to 5 mg/L, and then decreased with the initial concentrations increased (Figure 5). The result sustained was that the adsorbent material had a finite number of available sites on its specific surface, and they were occupied to the maximum when the sunscreen concentrations were raised. Thus, the absence of available sites on the AC surface obstructed the sunscreen compound removal at high concentrations within the aqueous medium.
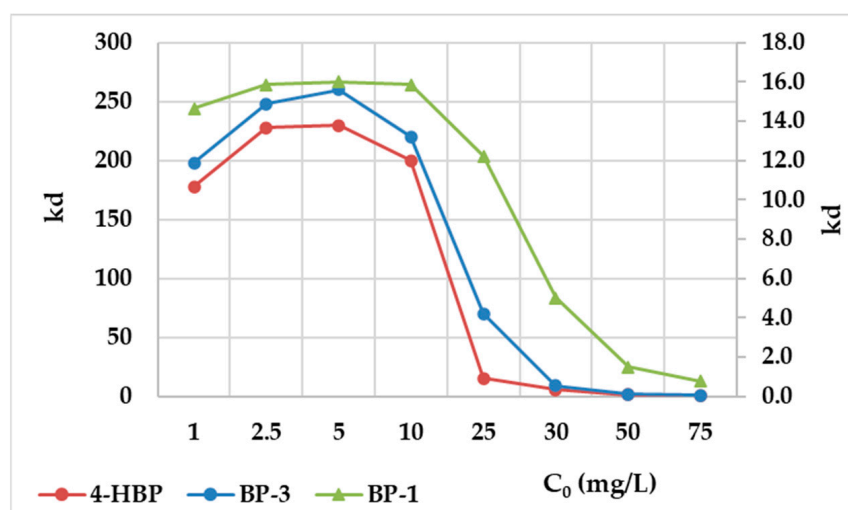
Figure 5. Graphical representation of distribution coefficients vs. initial sunscreen concentrations.

3.3. Adsorption Isotherms

In order to understand the adsorption mechanism and the equilibrium relations between the sunscreen concentrations and the amounts of sunscreen compounds accumulated on the available AC sites, the adsorbate–adsorbent relations were assessed by adsorption isotherms [28]. The adsorption data were plotted using two isotherm models, namely Langmuir and Freundlich. The basic postulate of the Langmuir model is that monolayer evolution takes place on the surface of adsorbent materials. It proved that a single organic molecule could be adsorbed on a single adsorption site, thus determining intermolecular forces to decrease with distance. Moreover, the Langmuir isotherm results assumed that the adsorbent material surface was homogenic, having energetically identical adsorption sites [28,41]. The Freundlich model describes a multilayer adsorption, involving adsorbent materials with heterogeneous surfaces, and is more of an empirical equation [42]. The Freundlich isotherm model describes the adsorption processes on heterogeneous surfaces and can be used to evaluate the adsorption equilibrium in non-monolayer surfaces [43]. The Freundlich model is an empirical equation which describes the adsorption of organic/inorganic molecules from an aqueous medium to a solid surface and presumes that various sites with different adsorption energies are implicated.

The Langmuir model showed the best match for all three sunscreen compounds, with correlation coefficient (R^2) values between 0.996 and 0.999 (Figure 6a). The adsorption capacities (mg/g) calculated using the Langmuir equation agreed well with the experimental values. The results suggest that the AC surface had monolayered coverage by the targeted sunscreen molecules [32]. The adsorption efficiencies (Qe) for 4-HBP, BP-3 and BP-1 are presented in Table 2 in the successive order: **BP-3** > **4-HBP** > **BP-1**. This order agrees with their log Kow values: **BP-3** (3.52) > **4-HBP** (3.07) > **BP-1** (2.96).

The adsorption efficiencies (Qe) for **4-HBP**, **BP-3** and **BP-1** are presented in Table 2 and have the successive order: **BP-3** > **4-HBP** > **BP-1**. This order agrees with their log Kow values: **BP-3** (3.52) > **4-HBP** (3.07) > **BP-1** (2.96). Higher adsorption efficiency values were determined for **BP-3** and **4-HBP**, compared with **BP-1**, and were expected given their higher log Kow values (3.52 and 3.07, respectively). Usually, chemical substances with higher log Kow values exhibit higher adsorption on the adsorbent materials [44]. This characteristic of compounds (log Kow) is directly proportional to any chemical substance's hydrophobicity and describes its higher predisposition to be adsorbed on a solid particle rather than remaining in an aqueous medium. The dimensionless separation factor (RL) was situated between 0 < RL < 1, suggesting that the adsorption process was a favorable one for all three sunscreen compounds (Table 3).
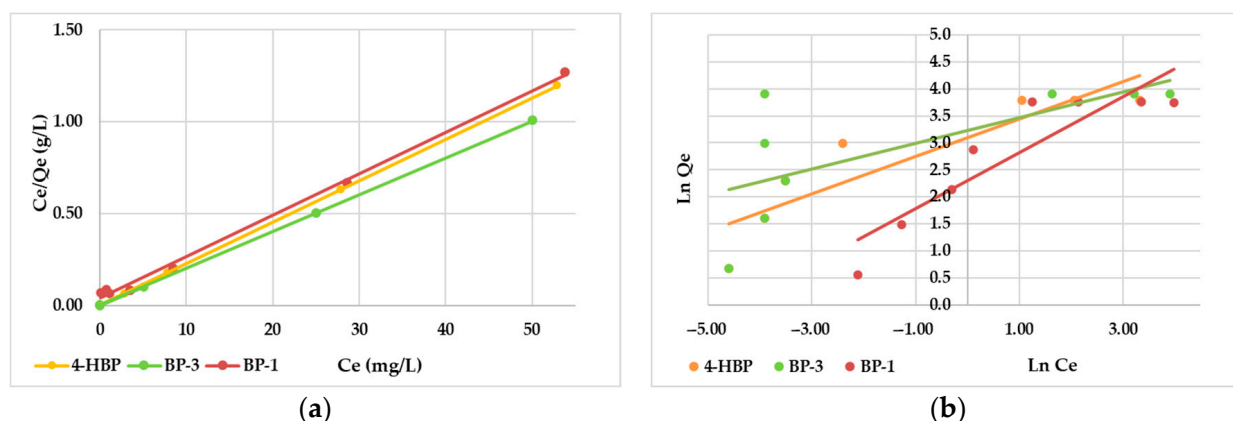
Figure 6. Langmuir (**a**) and Freundlich (**b**) adsorption isotherm models (pH 7; T, 25 °C; adsorbents, 0.025 g; volume, 50 mL; contact time, 10 h).

Table 3. Adsorption isotherm parameters.

Isotherm Model	4-HBP	BP-3	BP-1
Langmuir isotherm model			
Q_e (mg/g)	43.8	48.8	41.1
Q_m (mg/g)	44	49	44
K_L (L/mg)	9.81	10.5	0.57
R_L	0.0041	0.0038	0.0659
R^2	0.9999	0.9999	0.9964
Freundlich isotherm model			
K_F (mg/g)	22	28	20
1/n	0.3450	0.2625	0.5171
R^2	0.8119	0.4204	0.8209

Correlation coefficients obtained using the Freundlich model were much lower than those obtained from the Langmuir plots (Table 3), suggesting that Langmuir isotherms are the most suitable for describing the adsorption processes of the three targeted sunscreens onto the AC material. The constants *Kf* (slope) and n (intercept) were determined from the linear plot of ln*qe* vs. ln*Ce* (Figure 6b) and the obtained values are given in Table 2. The "n" value provides information regarding the level of non-linearity among solution concentrations and adsorptions: when n = 1, the adsorption was linear; when n < 1, the adsorption process was a chemical one, and when n > 1, the adsorption was a physical process [38]. In this study, the value of n was higher than the unit in all three cases (2.90 for **4-HBP**, 3.81 for **BP-3** and 1.93 for **BP-1**), suggesting a suitable adsorption process of sunscreens under the studied conditions. Although the correlation coefficients were lower than the ones obtained from the Langmuir isotherms, all results obtained from both isotherm models suggested that the adsorption of **4-HBP**, **BP-3** and **BP-1** onto the AC involved a monolayered distribution governed by physical interactions.

3.4. Adsorption Kinetic Studies

Adsorption kinetic studies are fundamental in optimizing the process conditions for the targeted molecules onto AC material. The adsorption kinetics of **4-HBP**, **BP-3** and **BP-1** were analyzed using two kinetic models: pseudo-first-order (PFO) and pseudo-second-order (PSO) (Figure 7).
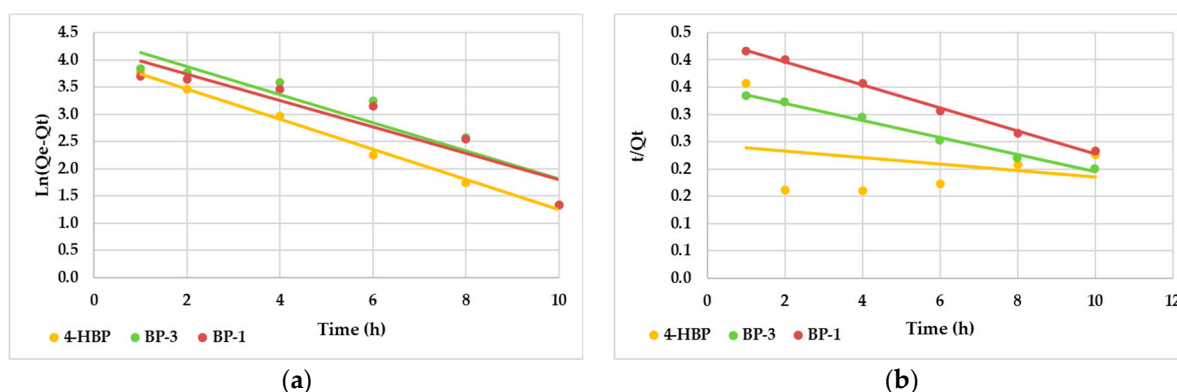
Figure 7. Plots of pseudo-first-order (**a**) and pseudo-second-order (**b**) kinetic models for the adsorption of the three sunscreen compounds onto AC at pH 7 and T = 25 °C.

The summary of the kinetic parameters of the three sunscreen compound adsorptions given in Table 3 revealed that the PFO kinetic model fit well the adsorption process of **4-HBP** (R^2 = 0.9922), while the PSO better described the adsorption processes of **BP-3** (R2 = 0.9908) and **BP-1** (R^2 = 0.9961) on the AC material. Thus, the obtained data suggest that the adsorption process could be physical sorption (electrostatic interaction or H bonding) for **4-HBP**. The pseudo-second-order kinetic model provided a better description of the adsorption process of **BP-3** and **BP-1** onto activated carbon. This model assumes that the rate-limiting step in the adsorption process is chemisorption, involving the exchange or sharing of electrons between the activated carbon and **BP-3**/**BP-1**. The model considers that the adsorption rate is directly related to the product of the concentrations of the activated carbon and **BP-3**/**BP-1** [9]. However, though the pseudo-second-order kinetic model provides important information about the rate of adsorption and can be used to determine the equilibrium adsorption capacity, it does not provide direct insights into the underlying mechanism of the adsorption process. The adsorption capacities of **4-HBP**, **BP-3** and **BP-1** onto AC at equilibrium (Qe) were 43.9, 52.6 and 47.2 mg/g, respectively, which were values close to the theoretical ones (Table 4).

Table 4. Kinetic model parameters.

Kinetic Model	4-HBP	BP-3	BP-1
Pseudo-first-order kinetic model			
Qe (mg/g) experimental	53.9	80.4	68.1
Q (mg/g) theoretical	44.3	49.9	42.9
K_1 (L/mg)	0.028	0.026	0.024
R^2	0.9922	0.8177	0.8627
Pseudo-second-order kinetic model			
Qe (mg/g) experimental	163.9	52.6	47.2
K_2	0.0002	0.0007	0.0010
R^2	0.0798	0.9908	0.9961

### 3.5. Adsorption Thermodynamic Studies

The temperature influence on the adsorption of **4-HBP**, **BP-3** and **BP-1** onto the commercial AC was studied through three thermodynamic parameters: Gibbs free energy (ΔG°), enthalpy (ΔH°) and entropy (ΔS°) changes. The thermodynamic parameters calculated for the adsorption of sunscreen compounds at different temperatures (25, 35, and 45 °C) are given in Table 5.

Table 5. Thermodynamic parameters for the three sunscreen compound adsorptions onto AC.

Sunscreen	Temperature (K)	K_L (L/mg)	K_L^0 (Dimensionless)	ΔG^0 (kJ/mol)	ΔH^0 (kJ/mol)	ΔS^0 (J/molK)
4-HBP	298	9.80	32.1	−10.8	−3209	25.7
	308	12.9	42.2	−11.1		
	318	18.5	60.6	−11.4		
BP-3	298	10.5	34.4	−13.5	−4590	30.5
	308	18.2	59.6	−13.8		
	318	28.9	94.6	−14.1		
BP-1	298	0.6	1.96	−22.7	−9092	42.7
	308	1.58	5.17	−23.1		
	318	4.09	13.39	−23.5		

$\Delta G°$ gives important information about the spontaneity of the process. $\Delta G°$ values were negative, being situated between −10.8 and −11.4 kJ/mol for **4-HBP**, between −13.5 and −14.1 11.4 kJ/mol for **BP-3**, and between −22.7 and −23.5 11.4 kJ/mol for **BP-1**, indicating that the adsorption process of the targeted sunscreen compounds on AC material was spontaneous. The decrease in $\Delta G°$ with growing temperature suggested that the process began to be thermodynamically unfavorable at superior temperatures [28]. For the three sunscreens, the obtained $\Delta G°$ values were situated below −20 kJ/mol or very closely to this reference value, indicating electrostatic relations between the target compounds and the AC material, which supports the physisorption mechanism. Usually, for the adsorption mechanism to be fixed with physical adsorption (electrostatic interaction), $\Delta G°$ values must be situated between 0 and −20 kJ/mol. Also, if charge transfer or coordinate bonds (chemisorption) are involved, more negative $\Delta G°$ values (−80 to −400 kJ/mol) are needed [45].

The linear graphical representation of $\ln K_L^0$ vs. $1/T$ is shown in Figure 8. The $\Delta H°$ values were assessed to be -3209 kJ/mol for **4-HBP**, −4590 kJ/mol for **BP-3** and −9092 kJ/mol for **BP-1**, while the entropy changes ($\Delta S°$) were estimated as 25.7 J/molK for **4-HBP**, 30.5 J/molK for **BP-3** and 42.7 J/molK for **BP-1** (Table 4), for the temperatures situated in the range of 25–45 °C. The negative results obtained for $\Delta H°$ indicate that the adsorption advanced well at lower temperatures and the adsorption mechanism was exothermic. The positive values obtained for $\Delta S°$ suggest that the freedom degree growth (or disorder) of the adsorbed **4-HBP**, **BP-3** and **BP-1** onto the commercial AC material was not restricted. In conclusion, the thermodynamic results suggest a spontaneous and exothermic adsorption process, indicating that physical interactions were involved [40].
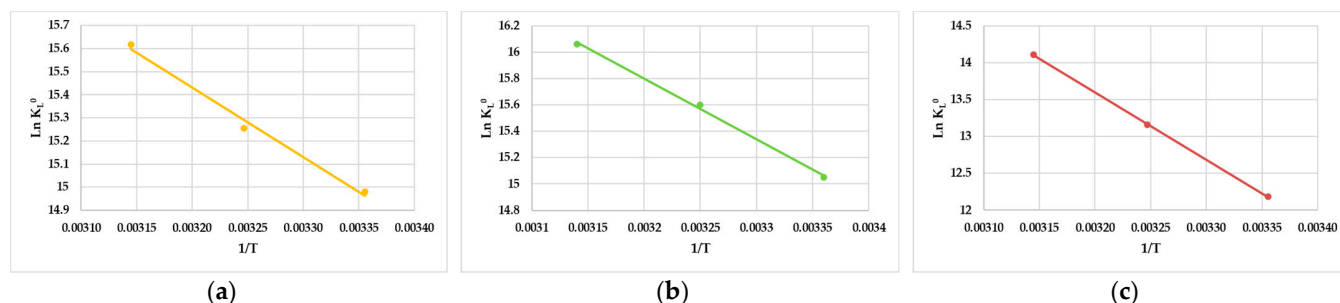
Figure 8. Plots of $\ln K_L^0$ vs. $1/T$ for (**a**) **4-HBP**, (**b**) **BP-3** and (**c**) **BP-1** adsorption on the commercial AC.

3.6. Elimination of Targeted Sunscreens from Actual Wastewater Samples

Optimal batch characteristics were used to determine the adsorption of the three target sunscreen compounds from five actual wastewater sample. Composite effluent samples with 24 h flow were collected in August 2023, during two consecutive days, from five wastewater treatment plants, serving the cities of Bucharest, Iasi, Ramnicu-Valcea,

Targoviste and Galati. The physicochemical properties of the wastewater samples were the following: pH, 6.8–7.3; temperature, 20.2–22.1 °C; conductivity, 1523–2315 μS/cm; BOD, 32–48; COD, 105–158; TSS, 16–32 mg/L; TN, 2.6–4.2 mg/L; NH_3–N, 31.4–44.8 mg/L; TP, 0.54–0.82 mg/L; PO_4^{3-}, 1.16–1.84 mg/L; and oil/fats, 12.4–18.2 mg/L. All samples were analyzed prior to the experiments having begun, and the results showed undetectable values of the target compounds. Thus, the samples were spiked with **4-HBP**, **BP-3** and **BP-1** at a concentration level of 25 mg/L. Viability of commercial AC to eliminate the three sunscreens as well as the matrix influence for the wastewater under batch conditions were assessed. Further, LC–MS/MS was used to analyze the wastewater samples, and the results are given in Table 6.

Table 6. Concentrations (±RSD, n = 3) of the targeted sunscreens obtained after the adsorption process.

Sample	4-HBP	BP-3 (mg/L ± RSD)	BP-1
S1	5.15 ± 0.12	1.20 ± 0.03	5.70 ± 0.15
S2	8.65 ± 0.20	5.20 ± 0.14	7.93 ± 0.21
S3	5.63 ± 0.13	1.90 ± 0.05	4.68 ± 0.13
S4	9.93 ± 0.23	6.20 ± 0.16	8.55 ± 0.23
S5	4.10 ± 0.09	3.13 ± 0.08	5.15 ± 0.14

Figure 9 shows the results obtained for the five samples after the adsorption process. The removal efficiencies were situated between 60.3% and 83.6% for **4-HBP**, between 75.2% and 95.2% for **BP-3**, and between 65.8 and 81.3% for **BP-1**.
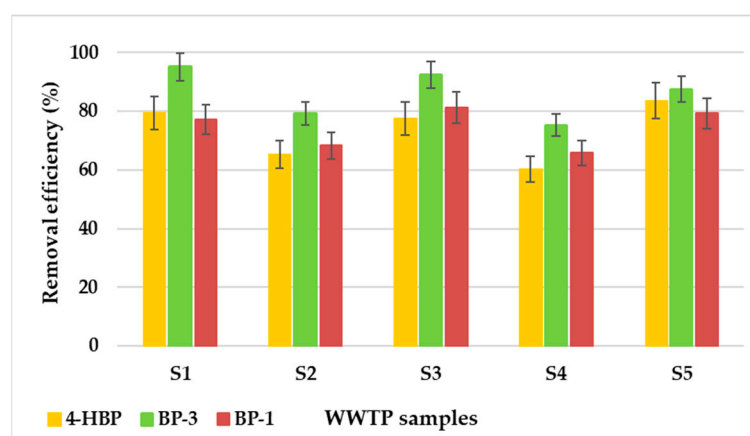

Figure 9. Comparative removal efficiencies of the targeted sunscreens from the wastewater samples using the AC material.

It was noticed that the removal efficiencies of the three sunscreen compounds decreased in comparison with the data acquired from the batch mode experiments. The phenomena responsible for these results may be the matrix effects and organic carbon amounts contained in the real WWTP samples. Thus, it can be concluded that the removal of the target sunscreen compounds from wastewater may be interfered with by the occurrence of other organic contaminants in the wastewater sample, which will compete for the free adsorption sites on the AC surface.

4. Discussion

The present study presents, for the first time, results regarding the removal of benzophenone-type sunscreen compounds from aqueous media by adsorption onto activated carbon. The lack of literature data regarding the adsorption of these types of organic pollutants on activated carbon makes it impossible to compare the results obtained with those obtained in other studies. However, a comparison with the results

obtained using other adsorbent materials was made. The most used compound for conducting adsorption studies in the literature was **BP-3**. To remove it from aqueous samples, the adsorbent materials used were the following: lipophilic organo-silicate, laponite and montmorillonite [28], different types of carbon materials (granular activated carbon, powered activated carbon and carbon nanotubes) [46], metal–organic framework (MOF) [16,47] and nanomaterials. Under optimal conditions, the adsorbed quantities of **BP-3** were 340 mg/g on organo-silicate, 137 mg/g on laponite and 192.3 mg/g montmorillonite [28]. Using different carbon-based materials, the results revealed good adsorption capacity on **BP-3**, the highest being 450.36 mg/g, being obtained for power-activated carbon [46]. Using different types of MOFs, the highest oxybenzone adsorption capacities were 560 mg/g [16], 73.50 mg/g and 120 mg/g, respectively [47].

To the best of our knowledge, the removal of **4-HBP** and **BP-1** using adsorption processes was not investigated until now. The data acquired in the present research offers promising data regarding the removal of three benzophenone-type sunscreen compounds from aqueous samples through adsorption onto activated carbon. The target substances represented are of high concern due to their aquatic environmental pollution and real threat to aquatic organisms. This study proposes a highly efficient, cost-effective and eco-friendly removal method for the elimination of three sunscreen compounds from wastewater samples, using commercial activated carbon.

Commercial activated carbon has proven to be a suitable adsorbent material for the removal of benzophenone-type target compounds from aqueous samples, this material being used in recent studies for the successful removal of other classes of organic pollutants from aqueous samples (pharmaceuticals and synthetic dyes). The removal of four nonsteroidal anti-inflammatory drugs, namely, ibuprofen, acetaminophen, diclofenac and ketoprofen from wastewater using the same AC material showed very satisfying results, with removal efficiencies varying between 88 and 98% and maximum adsorption capacities in the range of 0.64–0.85 mg/g [20]. Another study used commercial activated carbon to eliminate methyl orange from aqueous solutions. The maximum adsorption capacity was determined as 129.8 mg of methyl orange on 1 g of AC, with the highest removal of 97.8% [21]. Thus, previous studies have demonstrated that the adsorbent material used is a versatile one, able to remove different classes of organic pollutants (anti-inflammatory drugs up to 98%, synthetic dyes up to 97.8% and sunscreen compounds up to 99.9%) from aqueous media, and it can be regenerated and reused with high efficiency, with up to five reuse cycles [20,21].

The used AC adsorbent material is a common material with a low cost, energy savings, environmental friendliness and ease of recovery and recyclability. All this has led to a sustainable process for the elimination of organic compounds.

5. Conclusions

The adsorption of three benzophenone-type compounds onto commercial AC was researched and their equilibrium isotherms, kinetics and thermodynamics were studied. The data of the batch adsorption experiments revealed that the upper limit percentages of 88.6% for **4-HBP**, 99.9% for **BP-3** and 86.5% for **BP-1** removal were achieved at a 25 mg/L initial concentration, after 10 h, at pH 7, using 0.025 g of AC, at 25 °C, and with a 25 mL volume of the solution. The general investigation of the equilibrium model examinations indicated the fitting of Langmuir isotherm models to sunscreen–AC adsorption systems, which indicated an adsorption of the sunscreen compounds in monolayers onto the activated carbon surface. The kinetics results certified that the pseudo-first order kinetic model could describe the **4-HBP**-AC adsorption system, while the PSO kinetic could explain the adsorption of **BP-3** and **BP-1** onto the AC material. As a result, according to the kinetic models, it can be assumed that the retention of the 4-HBP contaminant on AC could have been due to physical interactions, while the retention of **BP-1** and **BP-3** on AC could have been achieved following chemical interactions. The sunscreen compound adsorption capacity of AC was noticed to be reducing when the temperature was increased, therefore,

being a sign that an exothermic adsorption process was occurring. The negative ΔG° values suggest a spontaneous adsorption process of target sunscreen compounds onto AC. The isotherm data and thermodynamic results achieved all confirm that the mechanisms of the adsorption of **4-HBP**, **BP-3** an **BP-1** on the AC surface were mostly electrostatic interactions, sustaining the physical sorption mechanisms. The results are favorable for a sustainable method to remove organic micropollutants from wastewater and could be considered in improving the wastewater treatment process.

References

1. Peinado, F.M.; Ocón-Hernández, O.; Iribarne-Durán, L.M.; Vela-Soria, F.; Ubiña, A.; Padilla, C.; Mora, J.C.; Cardona, J.; León, J.; Fernández, M.; et al. Cosmetic and personal care product use, urinary levels of parabens and benzophenones, and risk of endometriosis: Results from the EndEA study. *Environ. Res.* **2021**, *196*, 110342. [CrossRef]
2. Song, J.; Na, J.; An, D.; Jung, J. Role of benzophenone-3 additive in chronic toxicity of polyethylene microplastic fragments to Daphnia magna. *Sci. Total. Environ.* **2021**, *800*, 149638. [CrossRef]
3. Kim, S.; Choi, K. Occurrences, toxicities, and ecological risks of benzophenone-3, a common component of organic sunscreen products: A mini-review. *Environ. Int.* **2014**, *70*, 143–157. [CrossRef]
4. Hu, L.-X.; Cheng, Y.-X.; Wu, D.; Fan, L.; Zhao, J.-H.; Xiong, Q.; Chen, Q.-L.; Liu, Y.-S.; Ying, G.-G. Continuous input of organic ultraviolet filters and benzothiazoles threatens the surface water and sediment of two major rivers in the Pearl River Basin. *Sci. Total. Environ.* **2021**, *798*, 149299. [CrossRef]
5. Tsui, M.M.P.; Leung, H.W.; Wai, T.C.; Yamashita, N.; Taniyasu, S.; Liu, W.; Lam, P.K.S.; Murphy, M.B. Occurrence, distribution and ecological risk assessment of multiple classes of UV filters in surface waters from different countries. *Water Res.* **2014**, *67*, 55–65. [CrossRef]
6. Carstensen, L.; Zippel, R.; Fiskal, R.; Börnick, H.; Schmalz, V.; Schubert, S.; Schaffer, M.; Jungmann, D.; Stolte, S. Trace analysis of benzophenone-type UV filters in water and their effects on human estrogen and androgen receptors. *J. Hazard. Mater.* **2023**, *456*, 131617. [CrossRef]
7. Carstensen, L.; Beil, S.; Börnick, H.; Stolte, S. Structure-related endocrine-disrupting potential of environmental transformation products of benzophenone-type UV filters: A review. *J. Hazard. Mater.* **2022**, *430*, 128495. [CrossRef]
8. Moradi, N.; Amin, M.M.; Fatehizadeh, A.; Ghasemi, Z. Degradation of UV-filter Benzophenon-3 in aqueous solution using TiO2 coated on quartz tubes. *J. Environ. Health Sci. Eng.* **2018**, *16*, 213–228. [CrossRef]
9. Saif, S.; Adil, S.F.; Khan, M.; Hatshan, M.R.; Khan, M.; Bashir, F. Adsorption Studies of Arsenic(V) by CuO Nanoparticles Synthesized by *Phyllanthus emblica* Leaf-Extract-Fueled Solution Combustion Synthesis. *Sustainability* **2021**, *13*, 2017. [CrossRef]
10. Sabzehmeidani, M.M.; Mahnaee, S.; Ghaedi, M.; Heidari, H.; Roy, V.A.L. Carbon based materials: A review of adsorbents for inorganic and organic compounds. *Mater. Adv.* **2021**, *2*, 598–627. [CrossRef]
11. Du, E.; Li, J.; Zhou, S.; Li, M.; Liu, X.; Li, H. Insight into the Degradation of Two Benzophenone-Type UV Filters by the UV/H2O2 Advanced Oxidation Process. *Water* **2018**, *10*, 1238. [CrossRef]
12. Gong, P.; Yuan, H.; Zhai, P.; Xue, Y.; Li, H.; Dong, W.; Mailhot, G. Investigation on the degradation of benzophenone-3 by UV/H2O2 in aqueous solution. *Chem. Eng. J.* **2015**, *277*, 97–103. [CrossRef]
13. Hopkins, Z.R.; Snowberger, S.; Blaney, L. Ozonation of the oxybenzone, octinoxate, and octocrylene UV-filters: Reaction kinetics, absorbance characteristics, and transformation products. *J. Hazard. Mater.* **2017**, *338*, 23–32. [CrossRef]

14. Lee, Y.M.; Lee, G.; Kim, M.K.; Zoh, K.D. Kinetics and degradation mechanism of Benzophenone-3 in chlorination and UV/chlorination reactions. *Chem. Eng. J.* **2020**, *393*, 124780. [CrossRef]

15. Bhadra, B.N.; Yoo, D.K.; Jhung, S.H. Carbon-derived from metal-organic framework MOF-74: A remarkable adsorbent to remove a wide range of contaminants of emerging concern from water. *Appl. Surf. Sci.* **2020**, *504*, 144348. [CrossRef]

16. Wang, T.; He, J.; Lu, J.; Zhou, Y.; Wang, Z.; Zhou, Y. Adsorptive removal of PPCPs from aqueous solution using carbon-based composites: A review. *Chin. Chem. Lett.* **2022**, *33*, 3585–3593. [CrossRef]

17. Zhu, X.; He, M.; Sun, Y.; Xu, Z.; Wan, Z.; Hou, D.; Alessi, D.S.; Tsang, D.C.W. Insights into the adsorption of pharmaceuticals and personal care products (PPCPs) on biochar and activated carbon with the aid of machine learning. *J. Hazard. Mater.* **2022**, *423 Pt B*, 127060. [CrossRef]

18. Elias, K.D.; Ejidike, I.P.; Mtunzi, F.M.; Pakade, V.E. Endocrine Disruptors-(estrone and β-estradiol) removal from water by Nutshell activated carbon: Kinetic, Isotherms and Thermodynamic studies. *Chem. Thermodyn. Therm. Anal.* **2021**, *3–4*, 100013. [CrossRef]

19. Pirvu, F.; Covaliu-Mierla, C.I.; Paun, I.; Paraschiv, G.; Iancu, V. Treatment of Wastewater Containing Nonsteroidal Anti-Inflammatory Drugs Using Activated Carbon Material. *Materials* **2022**, *15*, 559. [CrossRef]

20. Serban, G.V.; Iancu, V.I.; Dinu, C.; Tenea, A.; Vasilache, N.; Cristea, I.; Niculescu, M.; Ionescu, I.; Chiriac, F.L. Removal Efficiency and Adsorption Kinetics of Methyl Orange from Wastewater by Commercial Activated Carbon. *Sustainability* **2023**, *15*, 12939. [CrossRef]

21. Zhou, Y.; Liu, X.; Xiang, Y.; Wang, P.; Zhang, J.; Zhang, F.; Tang, L. Modification of biochar derived from sawdust and its application in removal of tetracycline and copper from aqueous solution: Adsorption mechanism and modelling. *Bioresour. Technol.* **2017**, *245*, 266–273. [CrossRef] [PubMed]

22. Zietzschmann, F.; Stutzer, C.; Jekel, M. Granular activated carbon adsorption of organic micro-pollutants in drinking water and treated wastewater—Aligning breakthrough curves and capacities. *Water Res.* **2016**, *92*, 180–187. [CrossRef] [PubMed]

23. Sun, Y.; Yue, Q.; Gao, B.; Gao, Y.; Xu, X.; Li, Q.; Wang, Y. Adsorption and cosorption of ciprofloxacin and Ni(II) on activated carbon-mechanism study. *J. Taiwan Inst. Chem. Eng.* **2014**, *45*, 681–688. [CrossRef]

24. Boudrahem, N.; Delpeux-Ouldriane, S.; Khenniche, L.; Boudrahem, F.; Aissani-Benissad, F.; Gineys, M. Single and mixture adsorption of clofibric acid, tetracycline and paracetamol onto Activated carbon developed from cotton cloth residue. *Process. Saf. Environ. Prot.* **2017**, *111*, 544–559. [CrossRef]

25. Sbardella, L.; Comas, J.; Fenu, A.; Rodriguez-Roda, I.; Weemaes, M. Advanced biological activated carbon filter for removing pharmaceutically active compounds from treated wastewater. *Sci. Total. Environ.* **2018**, *636*, 519–529. [CrossRef]

26. Teixeira, S.; Delerue-Matos, C.; Santos, L. Application of experimental design methodology to optimize antibiotics removal by walnut shell based activated carbon. *Sci. Total. Environ.* **2019**, *646*, 168–176. [CrossRef]

27. Charaabi, S.; Tchara, L.; Marminon, C.; Bouaziz, Z.; Holtzinger, G.; Pensé-Lhéritier, A.-M.; Le Borgne, M.; Issa, S. A comparative adsorption study of benzophenone-3 onto synthesized lipophilic organosilicate, Laponite and montmorillonite. *Appl. Clay Sci.* **2019**, *170*, 114–124. [CrossRef]

28. Rossner, A.; Snyder, S.A.; Knappe, D.R.U. Removal of emerging contaminants of concern by alternative adsorbents. *Water Res.* **2009**, *43*, 3787–3796. [CrossRef]

29. Tran, T.; Dang, B.T.; Thuy, L.T.T.; Hoang, H.G.; Bui, X.T.; Le, V.G.; Lin, C.; Nguyen, M.K.; Nguyen, K.Q.; Nguyen, P.T.; et al. Advanced Treatment Technologies for the Removal of Organic Chemical Sunscreens from Wastewater: A Review. *Curr. Pollut. Rep.* **2022**, *8*, 288–302. [CrossRef]

30. Chiriac, F.L.; Paun, I.; Pirvu, F.; Iancu, V.; Galaon, T. Distribution, removal efficiencies and environmental risk assessment of benzophenone and salicylate UV filters in WWTPs and surface waters from Romania. *New J. Chem.* **2021**, *45*, 2478. [CrossRef]

31. Abril, D.; Ferrer, V.; Mirabal-Gallardo, Y.; Cabrera-Barjas, G.; Segura, C.; Marican, A.; Pereira, A.; Durán-Lara, E.F.; Valdés, O. Comparative Study of Three Dyes' Adsorption onto Activated Carbon from *Chenopodium quinoa* Willd and *Quillaja saponaria*. *Materials* **2022**, *15*, 4898. [CrossRef] [PubMed]

32. Rao, A.; Kumar, A.; Dhodapkar, R.; Pal, S. Adsorption of five emerging contaminants on activated carbon from aqueous medium: Kinetic characteristics and computational modeling for plausible mechanism. *Environ. Sci. Pollut. Res.* **2021**, *28*, 21347–21358. [CrossRef] [PubMed]

33. Chiriac, F.L.; Stoica, C.; Paun, I.; Pirvu, F.; Galaon, T.; Nita-Lazar, M. Biodegradation of two organic ultraviolet-filters by single bacterial strains. *Int. J. Environ. Sci. Technol.* **2023**, *20*, 9065–9076. [CrossRef]

34. Chiriac, F.L.; Lucaciu, I.E.; Paun, I.; Pirvu, F.; Gheorghe, S. In Vivo Bioconcentration, Distribution and Metabolization of Benzophenone-3 (BP-3) by *Cyprinus carpio* (European Carp). *Foods* **2022**, *11*, 1627. [CrossRef] [PubMed]

35. Scapin, E.; Maciel, G.P.d.S.; Polidoro, A.D.S.; Lazzari, E.; Benvenutti, E.V.; Falcade, T.; Jacques, R.A. Activated Carbon from Rice Husk Biochar with High Surface Area. *Biointerface Res. Appl. Chem.* **2021**, *11*, 10265–10277. [CrossRef]

36. Kumar, A.; Jena, H.M. High surface area microporous activated carbons prepared from Fox nut (*Euryale ferox*) shell by zinc chloride activation. *Appl. Surf. Sci.* **2015**, *356*, 753–761. [CrossRef]

37. Phele, M.J.; Ejidike, I.P.; Mtunzi, F.M. Adsorption efficiency of activated macadamia nutshell for the removal Organochlorine pesticides: Endrin and 4,4-DDT from aqueous solution. *J. Pharm. Sci. Res.* **2019**, *11*, 258–262.

38. Aljeboree, A.M.; Alshirifi, A.N.; Alkaim, A.F. Kinetics and equilibrium study for the adsorption of textile dyes on coconut shell activated carbon. *Arab. J. Chem.* **2017**, *10*, S3381–S3393. [CrossRef]

39. Rincon-Silva, N.G.; Moreno-Pirajan, J.C.; Giraldo, L. Equilibrium, kinetics and thermodynamics study of phenols adsorption onto activated carbon obtained from lignocellulosic material (*Eucalyptus Globulus* labill seed). *Adsorption* **2016**, *22*, 33–48. [CrossRef]

40. Machedi, S.; Ejidike, I.P.; Mtunzi, F.M.; Pakade, V.E.; Klink, M.J. Chlorinated Phenols Sorption Performance by Macadamia Activated Carbon and Grafted Macadamia Activated Carbon: Characterization, Kinetics, and Thermodynamic studies. *Orient. J. Chem.* **2019**, *35*, 1469–1479. [CrossRef]

41. Langmuir, I. The constitution and fundamental properties of solids and liquids. Part I. Solids. *J. Am. Chem. Soc.* **1916**, *38*, 2221–2295. [CrossRef]

42. AlOthman, Z.A.; Habila, M.A.; Ali, R.; Ghafar, A.A.; Hassouna, M.S.E. Valorization of two waste streams into activated carbon and studying its adsorption kinetics, equilibrium isotherms and thermodynamics for methylene blue removal. *Arab. J. Chem.* **2023**, *2*, 1148–1158. [CrossRef]

43. Freundlich, H.M.F. Über die Adsorption in Lösungen. *Z. Phys. Chem.* **1906**, *57U*, 385–470. [CrossRef]

44. Archana, G.; Dhodapkar, R.; Kumar, A. Ecotoxicological risk assessment and seasonal variation of some pharmaceuticals and personal care products in the sewage treatment plant and surface water bodies (lakes). *Environ. Monit. Assess.* **2017**, *189*, 446. [CrossRef] [PubMed]

45. Altıntıg, E.; Yenigun, M.; Sarı, A.; Altundag, H.; Tuzen, M.; Saleh, T.A. Facile synthesis of zinc oxide nanoparticles loaded activated carbon as an eco-friendly adsorbent for ultra-removal of malachite green from water. *Environ. Technol. Innov.* **2021**, *21*, 101305. [CrossRef]

46. Tengfei, C.H.U.; Dongdong, L.I.; Erdeng, D.U.; Wenhai, C.H.U.; Yingqing, G.U.O.; Naiyun, G.A.O. Adsorption characteristics and adsorption thermodynamics of typical UV sunscreen oxybenzone(BP-3)at trace level in water by carbon-based adsorption materials. *Acta Sci. Circumstantiae* **2016**, *3*, 865–872. [CrossRef]

47. Tumpa, N.F.; Jeong, Y.-K. Adsorptive Removal of a Pharmaceutical and Personal Care Product Oxybenzone from Water with "Metal-Organic Frameworks". *Asian Rev. Environ. Earth Sci.* **2018**, *5*, 1–7. [CrossRef]